

Effects of inorganic phosphate on endothermic force generation in muscle

K. W. Ranatunga

Department of Physiology, The School of Medical Sciences, University of Bristol, Bristol BS8 1TD, UK (k.w.ranatunga@bristol.ac.uk)

Using a rapid (*ca.* 0.2 ms) laser temperature jump technique, the rate of endothermic force generation was examined in single-skinned (rabbit psoas) muscle fibres when they were exposed to different levels of inorganic phosphate (a product released during ATP hydrolysis in active muscle). The steady force is reduced by increased phosphate but the apparent rate constant of force generation induced by a standard temperature jump (from *ca.* 9 °C to *ca.* 12 °C) increases two- to threefold when the phosphate added is increased from zero to *ca.* 25 mM. The increase in the apparent rate constant also exhibits saturation at higher phosphate levels and the relation is hyperbolic. Detailed examination of the data, particularly in relation to our pressure release experiments, leads to a scheme for the molecular steps involved in phosphate release and force generation in active muscle fibres, where phosphate release from attached cross-bridges involves three reversible and sequentially faster molecular steps. Step one is a moderately slow, pre-force generation step that probably represents a transition of cross-bridges from non-specific to stereospecific attached states. Step two is moderately fast and represents endothermic cross-bridge force generation (temperature sensitive) and step three is a very rapid phosphate release. Such a scheme accommodates findings from a variety of different studies, including pressure perturbation experiments and other studies where the effect of phosphate on muscle force was studied.

Keywords: endothermic force; phosphate release; temperature jump; tension transients; muscle force generation; pressure jump

1. INTRODUCTION

The basic event that underlies muscle contraction is an ATP-driven, cyclic interaction of cross-bridges (myosin heads) between thick (myosin, M) and thin (actin, A) filaments in a muscle sarcomere: active muscle force is generated from structural change(s) in the cross-bridges during their transient attachment to the thin filament (Huxley & Simmons 1971; Huxley 1985). However, the identity of the particular molecular step(s) in the ATPase hydrolysis pathway that underlies cross-bridge force generation remains unresolved. It has been inferred from several different studies that the release of inorganic phosphate (Pi) in the ATP hydrolysis pathway is closely coupled to active force generation in muscle fibres. This was proposed from our hydrostatic pressure release experiments (Fortune *et al.* 1991) and was supported by caged phosphate release experiments (Dantzig *et al.* 1992), as well as by experiments in which force responses to sinusoidal length perturbation were analysed (Zhao & Kawai 1994). The conclusion from these studies was that Pi release (binding) in muscle fibres is a two-step process and force generation is an isomerization of an acto-myosin complex (an attached cross-bridge) before Pi is released (*i.e.* an isomerization of the AM.ADP.Pi state).

A rapid temperature jump induces a tension rise with a characteristic time-course in maximally calcium-activated muscle fibres and a component of it is considered to be endothermic force generation in attached cross-bridges (Davis & Harrington 1987; Goldman *et al.* 1987;

Bershtitsky & Tsaturyan 1992). Indeed, it has been known for nearly half a century that the active force in mammalian muscle is very temperature sensitive, increasing several-fold in warming from low (*ca.* 5 °C) to high physiological (> 30 °C) temperatures (see Ranatunga 1994). However, the identity of the endothermic force generation remains unclear. First, Davis & Rogers (1995) provided some evidence from temperature jump experiments that endothermic force generation is only indirectly coupled to ATP hydrolysis and is an isomerization of acto-myosin complexes after Pi release (*i.e.* AM.ADP states). Second, recent X-ray data from frog fibres (Bershtitsky *et al.* 1997) has shown that structural changes underlying force generation following temperature jump and length perturbation are not equivalent. Third, the time-course of endothermic force generation at a given temperature was characteristically different in fast and slow skeletal muscle fibres (and in cardiac muscle fibres; Ranatunga 1997), indicating some coupling with the ATP pathway, but the fast-slow difference (three- to fourfold; Ranatunga 1996) was less than that obtained from Pi release experiments (> 30-fold; Millar & Homsher 1992). There has been no previous study on the effects of different levels of Pi on endothermic force generation. Therefore, we have examined the effects of added Pi on force generation induced by a standard laser temperature jump using previously described methodology (Ranatunga 1996).

Some aspects of this study were presented as abstracts to the European Muscle Conference (Ranatunga 1999a) and to the Biophysical Society Meeting (Ranatunga 1999b).

2. METHODS

Experiments were performed on chemically skinned (using 0.5% Brij) and glycerinated muscle fibres from rabbit psoas muscle. A single fibre was isolated (length 1–3 mm) and set up for tension recording in a trough assembly as described previously (Ranatunga 1994, 1996). A fibre was glued (using nitrocellulose) between two Invar hooks (low thermal expansion), one of which was attached to a force transducer (AE801, Akers; cut-beam design—resonant frequency 14 kHz) and the other to a motor. The trough assembly was mounted on an optical microscope stage and its temperature was kept at $< 10^{\circ}\text{C}$ by the cooling fluid, whereas the front trough temperature could be independently clamped by the thermoelectric modules (Peltier units) at a suitable temperature (*ca.* $9\text{--}10^{\circ}\text{C}$ in these experiments). Rapid temperature jumps of $2\text{--}3^{\circ}\text{C}$ were induced in the front trough by an infrared laser pulse (wave length $1.32\ \mu\text{m}$, duration 0.2 ms and maximum pulse energy *ca.* 2 J) obtained from a neodymium–yttrium–aluminium garnet (Nd-YAG) laser (Schwartz Electro-Optics, Inc., Florida, USA). The pulse entered through the front glass wall, was reflected by the aluminium back wall and heated the fibre and bathing buffer solution ($50\ \mu\text{l}$) in the trough. The solution temperature near the fibre (when monitored by a small thermocouple; see fig. 1 in Ranatunga (1996)) increased during the course of the laser pulse (*ca.* 0.2 ms) and remained elevated and constant for *ca.* 0.5 s following a laser temperature jump. The elevated temperature could be clamped for longer periods by means of small Peltier units assembled on the back trough wall. As in previous studies (Goldman *et al.* 1987), the buffer solutions contained glycerol-2-phosphate (G2P) as the pH buffer (chosen because of its low temperature sensitivity), but they also contained 4% Dextran 500 kDa to compress filament lattice spacing to normal dimensions. One solution with 25 mM added phosphate contained 8 mM Mg acetate, 5.5 mM ATP, 15 mM EGTA–CaEGTA, 8.8 mM creatine phosphate, 10 mM G2P, 10 mM glutathione and 25 mM K_2HPO_4 , while acetate replaced phosphate in adjusting the ionic strength in other solutions. The pH of the solutions was 7.1 and the ionic strength was *ca.* 190 mM. The initial sarcomere length of the muscle fibres was set to $2.5\ \mu\text{m}$. A muscle fibre was maximally Ca activated (pCa *ca.* 4) at $9\text{--}10^{\circ}\text{C}$ and a temperature jump was made at the tension plateau. The fibre was relaxed and the procedure was repeated with activations at different levels of added phosphate (range 0–25 mM).

The outputs of the tension transducer and the thermocouple were examined on a digital cathode ray oscilloscope and recorded using a PC-based computer (486, CENCE systems) with a CED 1401 (plus) laboratory interface (Cambridge Design Ltd, Cambridge, UK). The curve fitting to tension transients was done using a nonlinear curve-fitting program (FIG-P, Biosoft). A temperature jump resulted in a biphasic rise of tension (=force) above the pre-temperature jump level and a double exponential curve of the form $P_{\text{post}} - a_1 \exp(-(t-d)/\tau_1) - a_2 \exp(-(t-d)/\tau_2)$ was fitted to a tension transient, where P_{post} is the steady tension at high temperature (after the temperature jump), $a_{1,2}$ and $\tau_{1,2}$ are the amplitudes and time constants of the exponential components, t is the time and d is the time delay to the laser pulse. In a few transients, a temperature jump resulted in a small tension drop followed by a quick recovery towards the pre-temperature jump tension level before the biphasic tension rise above the pre-perturbation level (Davis & Rogers 1995; Ranatunga 1996). This small-amplitude initial recovery phase did not contribute to a tension rise above the pre-temperature jump tension level and its rate constant (*ca.*

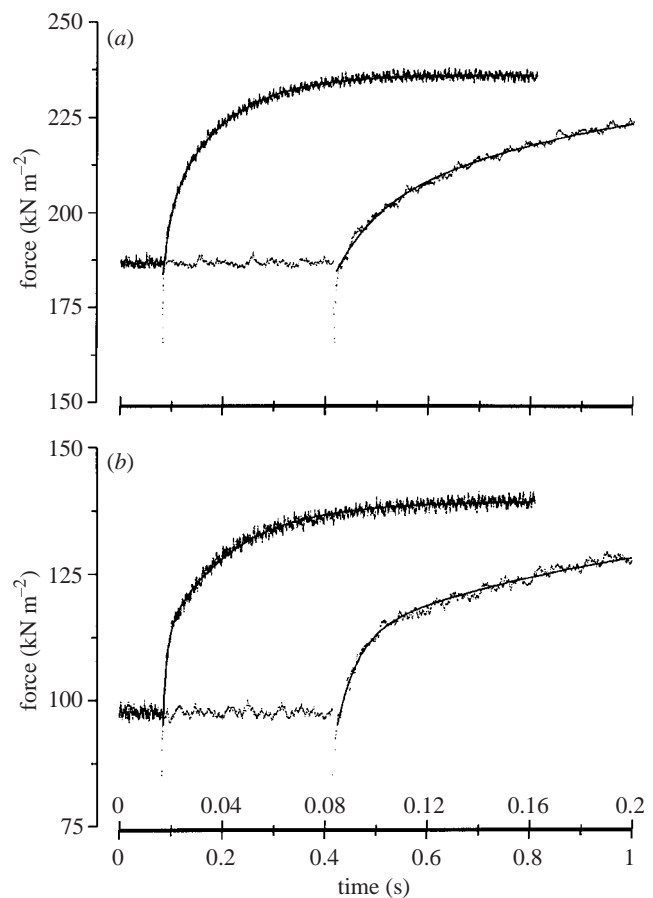


Figure 1. Sample records of tension (= force) transients induced by laser temperature jumps. The fibre (length 2.6 mm) was maximally calcium activated and a temperature jump of *ca.* 3°C was induced by a laser pulse at 80 ms after the beginning of each time trace (indicated by the downward spike (an artefact) on the tension trace). Each frame contains an individual tension transient, but it is illustrated at two different time-scales (upper and lower labelling on the x -axis). (a) Transient recorded after the fibre was activated in a medium containing no added phosphate (control). (b) Transient recorded after the fibre was relaxed and subsequently reactivated in a medium containing 12.5 mM added phosphate. The final temperature was $12.1\text{--}12.5^{\circ}\text{C}$. A bi-exponential curve is fitted to each transient to separate the two phases (phases 1 and 2) which constitute a transient: the exponential rates (\pm s.e. associated with the calculation) for phases 1 and 2 were (a) 66 ± 1.6 and $9.0 \pm 0.04\ \text{s}^{-1}$ for the control and (b) 123 ± 2.2 and $7.5 \pm 0.04\ \text{s}^{-1}$ with 12.5 mM added phosphate.

$500\ \text{s}^{-1}$) was not sensitive to added phosphate. Phases 1 and 2 in this study correspond to temperature jump relaxations 2 (slow) and 3 of Davis & Rodgers' (1995) analyses and phase 1 will be referred to as endothermic (cross-bridge) force generation.

3. RESULTS

Figure 1 shows sample records of the tension transients induced by the laser temperature jumps. The fibre was maximally calcium activated and a temperature jump of $2\text{--}3^{\circ}\text{C}$ was induced by a laser pulse: the transient in figure 1a was collected without added Pi and that in figure 1b was collected when the fibre was subsequently reactivated in the presence of 12.5 mM added Pi. It is seen that, compared to the control, the steady force

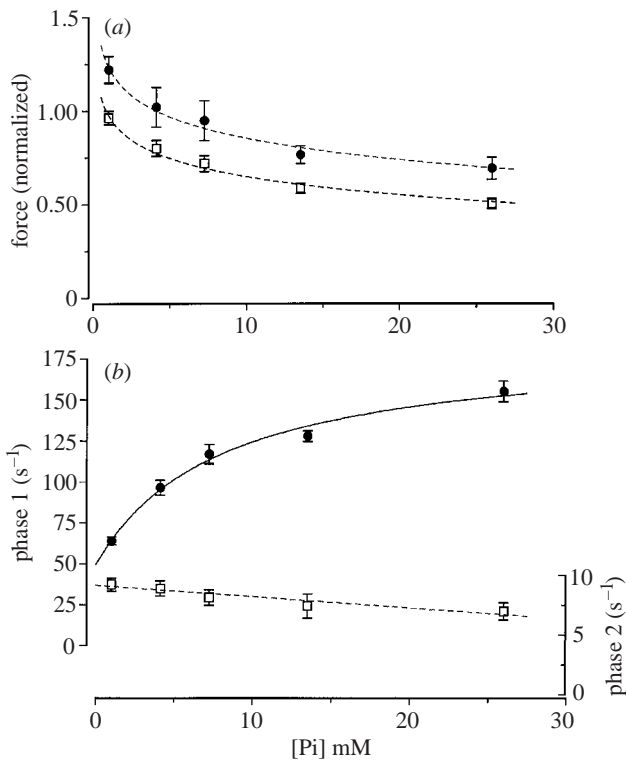


Figure 2. (a) Phosphate concentration dependence of steady active tension. A fibre was maximally calcium activated at *ca.* 9 °C (open squares) and temperature jumped to *ca.* 12 °C (filled circles). Pooled steady tension (mean \pm s.e.m.) data collected for the two temperatures (i.e. before and after a temperature jump) in five muscle fibres are shown. Tensions are normalized to that recorded in the first control active contraction in each fibre (i.e. with no added Pi at *ca.* 9 °C). A logarithmic curve is fitted to each data set as done in previous studies (see Cooke & Pate 1985; Dantzig *et al.* 1992). (Note that with no added Pi concentration, a control solution was assumed to contain *ca.* 1 mM Pi concentration due to contamination; Dantzig *et al.* 1992.) As is well-known, the active tension is depressed with an increase in Pi concentration: depression is 40–50% at 25 mM added Pi concentration in these experiments at 9–12 °C. (b) Phosphate dependence of the rate of endothermic force generation. The temperature jump tension transients in the above experiments were analysed by curve fitting as shown in figure 1 and the rate (reciprocal time constant) and the amplitude of each of the two exponential components determined. The mean (\pm s.e.m., $n = 7$ –15 per symbol) rates for the two phases are plotted against Pi concentration; filled symbols are data for phase 1 or endothermic force generation (left ordinate) and open symbols are data for phase 2 (right ordinate). The curve fitted to the phase 1 data is a hyperbolic equation of the form $\text{rate} = k_a + \{k_b \cdot [\text{Pi}] / (K_D + [\text{Pi}])\}$. The curve gives a value of $49.5 \pm 10.4 \text{ s}^{-1}$ for k_a (the forward rate constant of step I in scheme A), $135 \pm 6.0 \text{ s}^{-1}$ for k_b (the backward rate of step I) and $8.0 \pm 2.5 \text{ mM}$ for K_D (the dissociation constant for Pi release, step II in scheme A). The phase 2 rate is 5–10 s⁻¹ and it shows a slight decrease with Pi concentration: this may represent a contribution to tension rise of the cross-bridges going through a slow step in the cycle after the release of Pi.

before and after the temperature jump is smaller in the presence of Pi and the initial component of the tension rise (endothermic force generation) is faster in the presence of Pi.

Figure 2 shows the Pi dependence of steady active tension from five fibres. Each fibre was maximally calcium activated at *ca.* 9 °C (open squares) and temperature jumped to *ca.* 12 °C (filled circles). Pooled steady tension data (mean \pm s.e.m.) for the two temperatures (i.e. before and after a temperature jump) are shown where the tensions are normalized to that recorded in the first control active contraction (i.e. with no added Pi at *ca.* 9 °C). As is well-known, the active tension is depressed with an increase in Pi concentration (Cooke & Pate 1985): in these experiments the depression was 40–50% at 25 mM added Pi concentration at 9–12 °C. The tension transients induced by temperature jump in the experiments were analysed by curve fitting, as shown in figure 1 and the rate constant (reciprocal time constant) and amplitude of each of the two exponential components determined. The mean (\pm s.e.m.) apparent rate constants ($1/\tau_1$ and $1/\tau_2$) for the two phases are plotted against the phosphate concentration in figure 2b, where filled symbols are data for phase 1 (or endothermic force generation) and open symbols are data for the slower phase 2. It is seen that phase 2 shows minimal sensitivity to the level of phosphate added. On the other hand, the phase 1 rate constant increases with the phosphate concentration. The present data from five fibres showed that the rate constant increased from $64 \pm 2.4 \text{ s}^{-1}$ without added phosphate ($n = 15$) to $155 \pm 6.5 \text{ s}^{-1}$ with 25 mM added phosphate ($n = 8$). In addition, the data in figure 2b show that the rate constant exhibits saturation at high phosphate levels: the curve fitted to the phase 1 data in figure 2b is a hyperbola and it gives a maximum rate constant of 185 s^{-1} and an apparent dissociation constant for phosphate release of 8 mM.

It can be seen from the data in figure 2a that the steady tension versus phosphate concentration curves at low and high temperatures are approximately parallel: this indicates that the tension increase induced by a standard temperature jump remains similar. Figure 3a shows the amplitudes of the two components, plotted as percentages of the post-temperature jump steady tension (P_{post}) against the phosphate concentration. It can be seen from the mean data in figure 3a that the amplitude of each component with no phosphate added is 10–12% (i.e. 3–4% P_{post} per °C) and that the amplitudes are larger at increased phosphate concentrations. Indeed, the correlation between the percentage amplitudes and phosphate concentration was positive and significant for both phases ($r > 0.4$, $n = 46$ and $p < 0.005$).

4. DISCUSSION

As found in previous temperature jump studies, the net tension rise is biphasic (see Davis & Harrington 1987; Bershtsky & Tsaturyan 1992; Ranatunga 1996). The apparent rate constants for the two phases (with no added Pi) are 64 s^{-1} (phase 1) and *ca.* 10 s^{-1} (phase 2) at 12 °C and they are similar to the values of 69 s^{-1} and 14 s^{-1} obtained previously at 9–15 °C (Ranatunga 1996). The normalized amplitudes (3–4% P_{post} per °C) are also comparable (see fig. 7a in Ranatunga (1996)). The present results show that force depression by added Pi (figure 2a) is accompanied by a more rapid approach to equilibrium following a temperature jump (figure 2b). The apparent

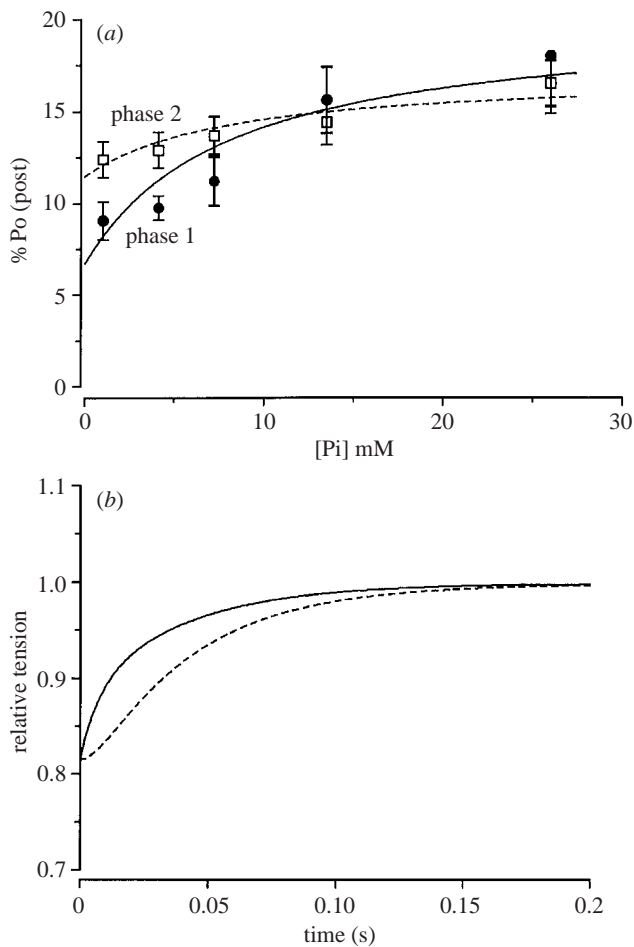


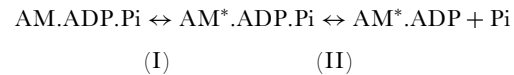
Figure 3. (a) Phosphate dependence of the amplitudes of the two phases. The mean (\pm s.e.m.) amplitudes of phase 1 (filled symbols) and phase 2 (open symbols) are plotted as percentages of the post-temperature jump tension on the ordinate and the curves are fitted by eye. Note that the normalized amplitudes are 10–12% with no added phosphate (1 mM) but tend to be larger (*ca.* 15%) at the higher phosphate concentrations; this is particularly noticeable in the amplitude data of phase 1 (endothermic force generation). (b) Two simulated tension transients. Pi release during cross-bridge cycling is assumed to involve three reversible and sequentially faster steps where force generation occurs during step II followed by rapid Pi release (step III in scheme B). The dotted curve represents force generation induced by perturbation of step I, assumed to be a pre-force generating step involving an increase in volume (and, hence, is pressure sensitive) and the curve is a tension transient induced by a simulated hydrostatic pressure release of *ca.* 15 MPa. The force generating step (step II) is assumed to be temperature sensitive and the solid curve represents a tension transient induced by a simulated temperature jump of *ca.* 3 °C. Note the different time-courses of the two transients, as obtained in the studies. The method used for simulation and other details are given in an accompanying paper by Gutfreund & Ranatunga (1999).

rate constant for phase 1 (endothermic force generation) increases and saturates at *ca.* 185 s^{-1} when the Pi concentration is increased to $> 25\text{ mM}$. Seemingly, these findings are at variance with those of Davis & Rogers (1995). They found that added Pi has a less marked effect on endothermic muscle force generation and concluded that cross-bridge force generation occurs in a step after the release of Pi. However, Davis & Rogers (1995) used

only one Pi concentration and their main concern in that study was examining the effect of added Pi over a wide range of temperatures.

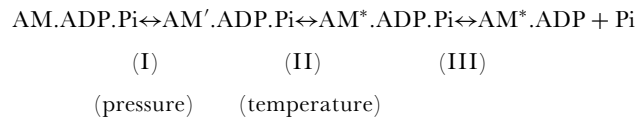
The phosphate dependence of endothermic force generation (phase 1) is basically similar to that which we reported for force generation following the release of hydrostatic pressure (pressure jump experiments) (Fortune *et al.* 1991) and is consistent with the general scheme (scheme A) shown below, where AM.X.X represent acto-myosin complexes (or attached cross-bridges) and phosphate (Pi) release involves at least two steps.

Scheme A:



The cross-bridge force generation represents a transition between two Pi-bound attached cross-bridge states (i.e. during step I above) before rapid Pi release in step II; this would lead to the hyperbolic relation obtained in the Pi dependence of phase 1 (see the caption to figure 2). However, the initial rate of tension rise (phase 1) in temperature jump experiments (64 s^{-1} with no added Pi and a maximum rate of 185 s^{-1}) is more than threefold higher than that obtained from pressure jump experiments (*ca.* 17 s^{-1} with no added Pi and a maximum rate of 52 s^{-1} at 12 °C). This discrepancy can be accounted for if Pi release in muscle fibres is assumed to involve at least three reversible steps, as shown in scheme B below.

Scheme B:



Step I is a moderately slow, pre-force generating step that involves a volume change (pressure sensitive), step II is a moderately fast, temperature-sensitive (endothermic), force generating step and step III is a rapid release of phosphate. According to the scheme, AM.ADP.Pi and AM'.ADP.Pi states are low-force states whereas AM*.ADP.Pi and AM*.ADP are high-force states. Whether such a three-step Pi release mechanism can accommodate the basic observations relating to cross-bridge force generation (phase 1) was examined by simulating temperature and pressure jumps applied to a simple AM.ATPase cycle that incorporated the linear kinetic scheme B above. Figure 3b shows the tension transients generated by simulation of a temperature jump (solid curve) and by simulation of a pressure jump (dotted curve): it is seen that a temperature jump tension transient is considerably faster than the pressure jump transient. It is interesting that the slower component (phase 2) of the tension transient, induced by temperature jump or pressure jump, is largely phosphate insensitive: in fact, its rate constant decreases slightly with added Pi (see figure 2b above and fig. 4d in Fortune *et al.* (1991)). It has been suggested that this reflects the presence of a rate-limiting step after the release of Pi in the cross-bridge cycle, but further work is necessary to identify the basis of this component. The method used for these simulations

and findings from them are given in more detail in a following paper (Gutfreund & Ranatunga 1999).

A basic scheme similar to scheme A was also proposed from analyses of the force decrease induced by Pi release from caged compounds (caged Pi release experiments) (Dantzig *et al.* 1992; Millar & Homsher 1992) and from analysis of complex moduli in experiments using a sinusoidal length perturbation technique (Zhao & Kawai 1994), both carried out on rabbit psoas fibres. The rate constant for force generation derived from those experiments, in which temperature was not perturbed, was *ca.* 20 s⁻¹ at 10–12 °C and corresponds to the forward rate of step I in scheme B (perturbation of step I as with pressure release). In general, scheme B can accommodate such findings and provide an explanation for the discrepancy observed between them (Millar & Homsher 1992; Zhao & Kawai 1994) and temperature jump studies (Ranatunga 1996) with respect to fast–slow fibre-type differences (see §1).

Interestingly, scheme B also provides a satisfactory interpretation for the more recent findings from X-ray diffraction measurements during heat-induced tension rise in muscle fibres (Bershtitsky *et al.* 1997). This study on frog fibres showed that the endothermic force generation was associated with a transition of the cross-bridges from a state where they are non-specifically attached to actin to one where cross-bridges are stereospecifically bound to actin. However, their data showed that the tension (=force) generation (1800 s⁻¹, frog fibre at 16–19 °C) was several times faster than the change in cross-bridge attached states (340 s⁻¹). Therefore, an alternative interpretation is that the signal monitored by X-ray diffraction (change of cross-bridge attached states) represents the slower pre-force generating step (step I in scheme B above) and is separate from the faster heat-induced endothermic force generation (step II in scheme B). An initial pre-force generating readjustment in attached cross-bridge states that precedes the force generation would also be consistent with findings where force generation has been linked to tilting of the light chain region of myosin heads (Irving *et al.* 1995), suggesting that the tilting represents step II in the scheme and, at constant temperature, it probably represents an entropic process. It would be of interest to examine the Pi dependence of force generation (recovery) induced by a length release. Because the sequential steps in scheme B are readily reversible, it is possible that, under some conditions, such transitions may occur in detached cross-bridges so that they may lead to ‘priming of cross-bridges for rapid force generation on attachment’ as recently reviewed and discussed by Huxley (1998).

I am grateful to the Wellcome Trust for its support of my research. I thank Professor Mike Geeves (University of Kent, UK) and Professor H. Gutfreund (University of Bristol, UK) for valuable comments and suggestions on the work and manuscript.

REFERENCES

- Bershtitsky, S. Y. & Tsaturyan, A. K. 1992 Tension responses to joule temperature jump in skinned rabbit muscle fibres. *J. Physiol.* **447**, 425–448.
- Bershtitsky, S. Y., Tsaturyan, A. K., Bershtitskaya, O. N., Mashanov, G. I., Brown, P., Burns, R. & Ferenczi, M. A. 1997 Muscle force is generated by myosin heads stereospecifically attached to actin. *Nature* **388**, 186–190.
- Cooke, R. & Pate, E. 1985 The effects of ADP and phosphate on the contraction of muscle fibers. *Biophys. J.* **48**, 789–798.
- Dantzig, J. A., Goldman, Y. E., Millar, N. C., Lactis, J. & Homsher, E. 1992 Reversal of the crossbridge force-generating transition by photogeneration of phosphate in rabbit psoas muscle fibres. *J. Physiol.* **451**, 247–278.
- Davis, J. S. & Harrington, W. 1987 Force generation by muscle fibres in rigor: a laser temperature-jump study. *Proc. Natl Acad. Sci. USA* **84**, 975–979.
- Davis, J. S. & Rogers, M. E. 1995 Indirect coupling of phosphate release to *de novo* tension generation during muscle contraction. *Proc. Natl Acad. Sci. USA* **92**, 10 482–10 486.
- Fortune, N. S., Geeves, M. A. & Ranatunga, K. W. 1991 Tension responses to rapid pressure release in glycerinated rabbit muscle fibres. *Proc. Natl Acad. Sci. USA* **88**, 7323–7327.
- Goldman, Y. E., McGray, J. A. & Ranatunga, K. W. 1987 Transient tension changes initiated by laser temperature jumps in rabbit psoas muscle fibres. *J. Physiol.* **392**, 71–95.
- Gutfreund, H. & Ranatunga, K. W. 1999 Simulation of molecular steps in muscle force generation. *Proc. R. Soc. Lond. B* **266**. (In the press.)
- Huxley, A. F. 1998 Biological motors: energy storage in myosin molecules. *Curr. Biol.* **8**, R485–R488.
- Huxley, A. F. & Simmons, R. M. 1971 Proposed mechanism of force generation in striated muscle. *Nature* **233**, 533–538.
- Huxley, H. E. 1985 The crossbridge mechanism of muscular contraction and its implications. *J. Exp. Biol.* **115**, 17–30.
- Irving, M., Allen, T. St C., Sabido-David, C., Craik, J. S., Brandmeir, B., Kendrick-Jones, J., Corrie, J. E. T., Trentham, D. R. & Goldman, Y. E. 1995 Tilting of the light-chain region of myosin during step length changes and active force generation in skeletal muscle. *Nature* **375**, 688–691.
- Millar, N. C. & Homsher, E. 1992 Kinetics of force generation and phosphate release in skinned rabbit soleus muscle fibers. *Am. J. Physiol.* **262**, C1239–C1245.
- Ranatunga, K. W. 1994 Thermal stress and Ca-independent contractile activation in mammalian skeletal muscle fibers at high temperatures. *Biophys. J.* **66**, 1531–1541.
- Ranatunga, K. W. 1996 Endothermic force generation in fast and slow mammalian (rabbit) muscle fibers. *Biophys. J.* **71**, 1905–1913.
- Ranatunga, K. W. 1997 Laser temperature jump experiments on mammalian (rat) cardiac muscle fibres. *J. Physiol.* **504.P**, 62P.
- Ranatunga, K. W. 1999a Endothermic force generation in mammalian muscle fibres: effects of inorganic phosphate. *J. Musc. Res. Cell Motil.* (In the press.)
- Ranatunga, K. W. 1999b Force generation and phosphate (Pi) release in muscle. *Biophys. J.* **76**, A160.
- Zhao, Y. & Kawai, M. 1994 Kinetic and thermodynamic studies of the cross-bridge cycle in rabbit psoas muscle fibers. *Biophys. J.* **67**, 1655–1668.

